is postulated to occur via intramolecular Michael reaction between the cationic enolate **4** and additional, coordinated monomer. The propagation step is analogous to that postulated to occur in group-transfer polymerization of acrylates, initiated by enol silanes in the presence of, for example, Lewis acid catalysts.[9]

Indirect evidence for the intermediacy of enolate **4** is based on the following observations. A mixture of compound **1** and $Cp_2Zr(OCH{=}CMe_2)Me$[10a] gives rise to compound **2** at the expense of both starting materials (Scheme I, eq 2), and this mixture is active for polymerization. The bis enolate complex, $Cp_2Zr[OC(OtBu){=}CMe_2]_2$,[10b] in the presence of 1 equiv of a proton source ($[Et_3NH][BPh_4]$),[10c] rapidly polymerizes methyl methacrylate (eq 4, Scheme I: 96% conversion after 30 min at 0 °C; M_n = 442 000, M_w/M_n = 1.14).

It is clear that the process described here is an efficient method for effecting high-conversion polymerization of methacrylate monomer to high molecular weight polymers with narrow molecular weight distributions. Work that is already in progress is designed to provide concrete evidence for the intermediacy of cationic enolate **4**, to investigate the kinetics of this process, and to evaluate whether polymer chains generated in this manner are living.

Acknowledgment. We thank the Natural Sciences and Engineering Research Council of Canada for financial support of this work. D.G.W. also thanks Polysar Rubber Corporation for a generous stipend.

Supplementary Material Available: Experimental details for the preparation of relevant compounds, polymerizations, and polymer characterization including GPC analyses (18 pages). Ordering information is given on any current masthead page.

(9) See, inter alia: (a) Webster, O. W. *Science* **1991**, *251*, 887. (b) Muller, A. H. E. *Makromol. Chem., Macromol. Symp.* **1990**, *32*, 87. (b) Sogah, D. Y.; Hertler, W. R.; Webster, O. W.; Cohen, G. M. *Macromolecules* **1987**, *20*, 1473. (c) Reetz, M. T.; Ostarek, R.; Piejko, K.-E.; Arlt, D. A.; Bomer, B. *Angew. Chem., Int. Ed. Engl.* **1986**, *25*, 1108. (d) Hertler, W. R.; Sogah, D. Y.; Webster, O. W.; Trost, B. M. *Macromolecules* **1984**, *17*, 1417.

(10) (a) Curtis, M. D.; Thanedar, S.; Butler, W. M. *Organometallics* **1984**, *3*, 1855. (b) See the supplementary material for the preparation and characterization of this compound. (c) Reaction of this compound with $[Et_3NH][BPh_4]$ in CD_2Cl_2 or THF-d_8 in the absence of monomer leads to the rapid appearance of a new species whose spectral features are consistent with a cationic enolate (see the supplementary material).

Regioselective C–N Bond Cleavage in an η^2(N,C)-Coordinated Pyridine and an η^1(N) → η^2(N,C) Bonding Rearrangement in Coordinated Quinoline: Models for Hydrodenitrogenation Catalysis

Steven D. Gray, David P. Smith, Michael A. Bruck, and David E. Wigley*

Carl S. Marvel Laboratories of Chemistry
Department of Chemistry, University of Arizona
Tucson, Arizona 85721

Received February 13, 1992

The catalytic removal of sulfur and nitrogen from petroleum feedstocks and coal-derived liquids is essential to preclude the poisoning of hydrocracking and reforming catalysts and to reduce emissions of their oxides.[1] Industrial hydrodenitrogenation (HDN) is typically effected over sulfided $CoMo/Al_2O_3$ or $NiMo/Al_2O_3$ under conditions which remove nitrogen as NH_3.[2,3]

(1) (a) Satterfield, C. N. *Heterogeneous Catalysis in Industrial Practice*; McGraw-Hill: New York, 1991. (b) Gates, B. C.; Katzer, J. R.; Schuit, G. C. A. *Chemistry of Catalytic Processes*; McGraw-Hill: New York, 1979.

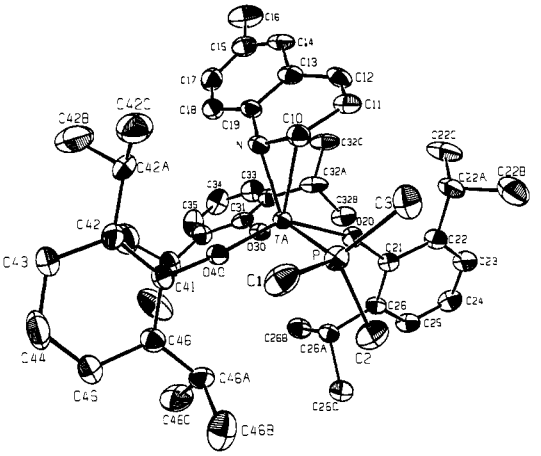

Figure 1. Molecular structure of (η^2(*N*,*C*)-6-methylquinoline)Ta(DIPP)$_3$(PMe_3) (**5**) (DIPP = O-2,6-$C_6H_3{}^iPr_2$). Selected interatomic distances (Å): Ta–N = 1.961 (7); Ta–C(10) = 2.208 (9); N–C(10) = 1.44 (1); C(10)–C(11) = 1.42 (1); C(11)–C(12) = 1.30 (1); C(12)–C(13) = 1.48 (2); C(13)–C(19) = 1.40 (1); N–C(19) = 1.41 (1). Selected bond angles (deg): Ta–N–C(19) = 145.0 (6); Ta–C(10)–C(11) = 123.4 (6); C(10)–Ta–N = 39.7 (3).

The nitrogen-containing compounds which are most difficult to process are the aromatic heterocycles such as pyridine, quinoline, and indole derivatives.[2,4] One central question in HDN catalysis which remains unresolved concerns how the strong C–N bonds in these heterocycles are cleaved.[5] Herein we provide evidence for an η^1(N) → η^2(N,C) bonding rearrangement in model HDN substrates and demonstrate that nucleophilic attack of an η^2(*N*,*C*)-pyridine results in facile, regioselective C–N bond cleavage.

Upon reaction of Ta(DIPP)$_3$Cl$_2$(OEt$_2$)[6] (**1**, DIPP = O-2,6-$C_6H_3{}^iPr_2$) with 1 equiv of quinoline (QUIN), yellow (QUIN)Ta(DIPP)$_3$Cl$_2$ (**2**) is isolated in ca. 95% yield (Scheme I). The analogous 6-methylquinoline (6MQ) adduct, (6MQ)Ta(DIPP)$_3$Cl$_2$ (**3**), is prepared similarly. NMR data[7] for **2** and **3** are entirely consistent with the heterocycle bonding η^1(N) to the d^0 metal center. Upon reduction of (η^1(*N*)-QUIN)Ta(DIPP)$_3$Cl$_2$ (**2**) with 2 equiv of NaHg, a dark red, *highly* soluble compound is obtained, for which spectroscopic data suggest the formulation (η^2(*N*,*C*)-QUIN)Ta(DIPP)$_3$ (**4**). In particular, the quinoline H(2) resonance at δ 9.63 in the ^{1}H NMR spectrum of **2** has shifted upfield to δ 4.07 in complex **4** (both in C_6D_6), diagnostic of the η^2(N,C) bonding mode.[8-10]

The crystalline, 6-methylquinoline adduct (η^2(*N*,*C*)-6MQ)Ta(DIPP)$_3$(PMe_3) (**5**) is afforded upon reducing **1** in the presence

(2) (a) Ho, T. C. *Catal. Rev.-Sci. Eng.* **1988**, *30*, 117. (b) Ledoux, M. J. In *Catalysis*; The Chemical Society: London, 1988; Vol. 7, pp 125–148.

(3) For example, see: (a) Fish, R. H.; Michaels, J. N.; Moore, R. S.; Heinemann, H. *J. Catal.* **1990**, *123*, 74 and references therein. (b) Olalde, A.; Perot, G. *Appl. Catal.* **1985**, *13*, 373. (c) Satterfield, C. N.; Yang, S. H. *Ind. Eng. Chem. Process Des. Dev.* **1984**, *23*, 11. (d) Fish, R. H.; Thormodsen, A. D.; Moore, R. S.; Perry, D. L.; Heinemann, H. *J. Catal.* **1986**, *102*, 270.

(4) (a) Fish, R. H. *Ann. N.Y. Acad. Sci.* **1983**, *415*, 292. (b) Laine, R. M. *Ibid.* **1983**, *415*, 271. (c) Laine, R. M. *Catal. Rev.-Sci. Eng.* **1983**, *25*, 459 and references therein.

(5) For discussion, see refs 2 and 4 and the following: Vivier, L.; Dominguez, V.; Perot, G.; Kasztelan, S. *J. Mol. Catal.* **1991**, *67*, 267.

(6) Strickler, J. R.; Bruck, M. A.; Wexler, P. A.; Wigley, D. E. *Organometallics* **1990**, *9*, 266.

(7) Spectroscopic and analytical data for compounds **2–5** and **7** are available as supplementary material. Partial ^{1}H NMR (in C_6D_6) for 6MQ H(2) resonances: **3** (333 K) δ 9.24 (br); **5** (probe temperature) δ 3.68 (br s).

(8) (a) Covert, K. J.; Neithamer, D. R.; Zonnevylle, M. C.; LaPointe, R. E.; Schaller, C. P.; Wolczanski, P. T. *Inorg. Chem.* **1991**, *30*, 2494. (b) Neithamer, D. R.; Párkányi, L.; Mitchell, J. F.; Wolczanski, P. T. *J. Am. Chem. Soc.* **1988**, *110*, 4421.

(9) Smith, D. P.; Strickler, J. R.; Gray, S. D.; Bruck, M. A.; Holmes, R. S.; Wigley, D. E. *Organometallics* **1992**, *11*, 1275.

(10) For an η^1(N) → $\eta^6(\pi)$ rearrangement in model ruthenium heterocycle compounds, see: (a) Fish, R. H.; Kim, H.-S.; Fong, R. H. *Organometallics* **1989**, *8*, 1375. (b) Fish, R. H.; Kim, H.-S.; Fong, R. H. *Ibid.* **1991**, *10*, 770.

0002-7863/92/1514-5462$03.00/0

Scheme I

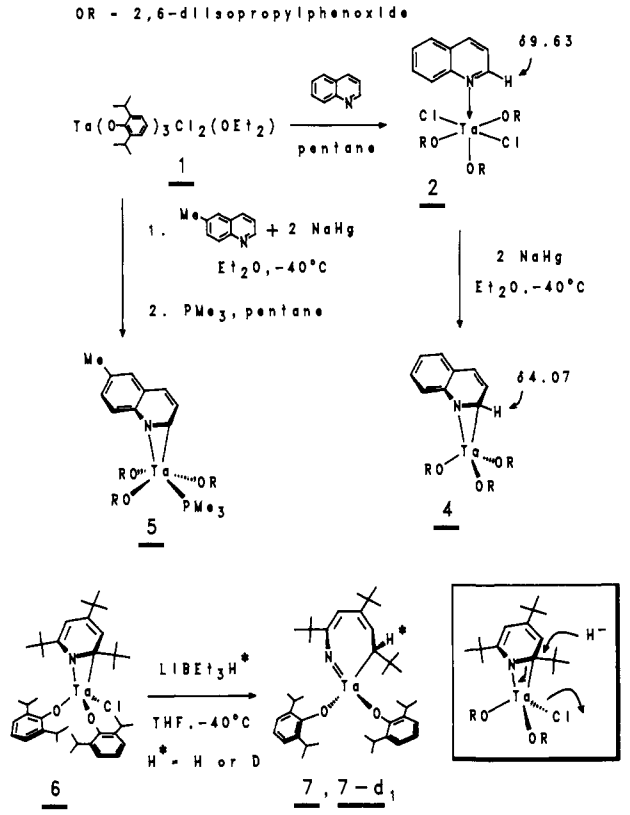

of 6MQ (first forming $(\eta^2(N,C)$-6MQ)Ta(DIPP)$_3$), followed by the addition of PMe_3 (Scheme I).[7] The X-ray structural determination[11] of **5** (Figure 1) confirms the η^2-(N,C) bonding mode of the heterocycle and provides evidence for the disruption of its aromaticity. The Ta–C(10) = 2.208 (9) Å, Ta–N = 1.961 (7) Å, and C(10)–N = 1.44 (1) Å bond distances imply the Ta(V) "metallaaziridine" formulation described previously.[8,9] Heterocycle distortions are evident from the π electron localization (C(11)–C(12) = 1.30 (1) Å) and from the location of N below and C(10) above the best 6MQ ligand plane.[12]

The pyridine complex $(\eta^2(N,C)$-2,4,6-$NC_5H_2{}^tBu_3)$Ta(DIPP)$_2$Cl (**6**)[9] also exhibits a Ta(V) metallaaziridine structure and can be considered a model HDN substrate → catalyst complex related to **4** and **5**. Upon reaction of **6** with $LiBEt_3H$, red crystals of compound **7** are obtained in moderate yield, along with LiCl (Scheme I). Spectroscopic data for **7** (and for **7**-d_1, prepared using $LiBEt_3D$) are consistent with hydride attack at the bound carbon of the $\eta^2(N,C)$-pyridine ligand, but X-ray crystallography provides the dramatic evidence that the nitrogen–carbon bond in the pyridine has been cleaved.

The molecular structure[13] of **7** (Figure 2) clearly reveals the

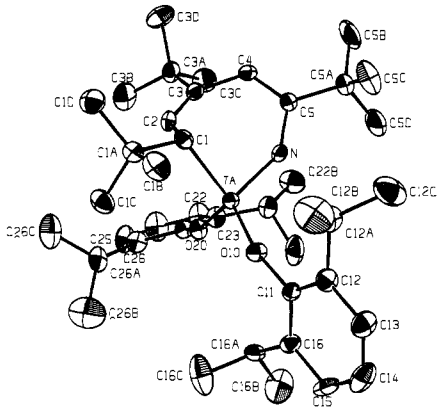

Figure 2. Molecular structure of (DIPP)$_2$Ta(=NC^{t}Bu=CHC^{t}Bu=CHCH^{t}Bu) (**7**) (DIPP = O-2,6-$C_6H_3{}^iPr_2$). Selected interatomic distances (Å): Ta–C(1) = 2.162 (9); C(1)–C(2) = 1.51 (1); C(2)–C(3) = 1.35 (1); C(3)–C(4) = 1.49 (1); C(4)–C(5) = 1.34 (1); C(5)–N = 1.40 (1); Ta–N = 1.779 (8); N–C(1) = 2.74 (1). Selected bond angles (deg): Ta–C(1)–C(2) = 89.2 (6); Ta–N–C(5) = 145.7 (6); C(1)–Ta–N = 87.6 (3).

disconnection between N and C(1) of the former $\eta^2(N,C)$-pyridine ligand and the resulting metallacyclic structure (DIPP)$_2$Ta(=NC^{t}Bu=CHC^{t}Bu=CHCH^{t}Bu) (**7**). Thus, in the metallaaziridine description of **6**, the former *amido* nitrogen has been transformed into a formal M=NR *imido* linkage (Ta—N = 1.779 (8) Å) upon hydride attack (Scheme I). The Ta—N—C(5) angle of 145.7 (6)° represents a strongly bent terminal imide which clearly arises from the constraints of the metallacycle, including the sp^3 hybridization of C(1).

This demonstration of C–N bond cleavage is consistent with the proposal that nucleophilic attack on a *coordinated* heterocycle effects C–N bond scission in HDN,[4b,c] thus providing an alternative explanation of how H_2S (or $[SH]^-$) arising from HDS actually enhances the rate of HDN.[14,15] One feature of this system, which contrasts with osmium η^2 heterocycles such as $[(\eta^2(C,C)$-lutidene)Os$(NH_3)_5]^{2+}$,[16] is that d^2 tantalum prefers to bind nitrogen heterocycles primarily in the η^2(N,C) mode,[8a] thereby selectively activating the heterocyclic ring.[17]

Acknowledgment is made to the National Science Foundation (CHE-8919367) for support of this research. We also thank the Materials Characterization Program (State of Arizona) for partial support, Dr. Richard H. Fish (Lawrence Berkeley Laboratory) for helpful discussions, and Mark Malcomson and Kevin Allen for invaluable experimental assistance.

Supplementary Material Available: Listings of spectroscopic data for compounds **2**–**5** and **7** and full details of the structure solution and crystallography for $(\eta^2(N,C)$-6-methylquinoline)Ta(DIPP)$_3$(PMe$_3$) (**5**) and (DIPP)$_2$Ta(=NC^{t}Bu=CHC^{t}Bu=CHCH^{t}Bu) (**7**), including tables of atomic positional and thermal parameters, bond distances and angles, least-squares planes, and dihedral angles and ORTEP figures (40 pages); tables of observed and calculated structure factor amplitudes (47 pages). Ordering information is given on any current masthead page.

(11) Crystal data for $C_{49}H_{69}NO_3PTa$ (**5**): yellow, monoclinic, $C2_1/c$ (No. 15); a = 32.849 (3) Å, b = 19.579 (2) Å, c = 23.822 (2) Å, β = 135.69 (49)°; V = 10702 (2) Å^3 for Z = 8 and FW = 932.02; D(calcd) = 1.16 g cm^{-3}, μ(Mo Kα) = 20.9 cm^{-1} (T = 20 ± 1 °C). A total of 10919 reflections (9393 unique) with a maximum 2θ = 50.0° were collected, of which 5289 reflections with $F_o^2 > 3.0\sigma(F_o^2)$ were used in the refinement; R = 0.054; R_w = 0.087. **5** crystallized with partial solvent occupation of the lattice, thereby limiting the overall precision of the structure.

(12) Consistent with this disruption of aromaticity is the fact that **4** hydrogenates to 1,2,3,4-tetrahydroquinoline under conditions (125 psi of H_2, room temperature) where **2** or free QUIN itself are unreactive. This hydrogenation also produces some biquinoline. See: Chiang, L. Y.; Swirczewski, J. W.; Kastrup, R.; Hsu, C. S.; Upasani, R. B. *J. Am. Chem. Soc.* **1991**, *113*, 6574.

(13) Crystal data for $C_{41}H_{64}NO_2Ta$ (**7**): red, monoclinic, $P2_1/n$ (No. 14); a = 21.150 (2) Å, b = 9.623 (1) Å, c = 21.519 (2) Å, β = 108.63 (18)°; V = 4150.5 Å^3 for Z = 4 and FW = 783.92; D(calcd) = 1.25 g cm^{-3}, μ(Mo Kα) = 26.5 cm^{-1} (T = 20 ± 1 °C). A total of 8037 reflections (7324 unique) with a maximum 2θ = 50.0° were collected, of which 4091 reflections with $F_o^2 > 3.0\sigma(F_o^2)$ were used in the refinement: R = 0.040, R_w = 0.049. The proton attached to C(1) was also located in the difference map.

(14) (a) Satterfield, C. N.; Gültekin, S. *Ind. Eng. Chem. Process Des. Dev.* **1981**, *20*, 62. (b) Yang, S. H.; Satterfield, C. N. *Ibid.* **1984**, *23*, 20. (c) Yang, S. H.; Satterfield, C. N. *J. Catal.* **1983**, *81*, 168 and references therein. (d) Brunet, S.; Perot, G. *React. Kinet. Catal. Lett.* **1985**, *29*, 15.

(15) This rate enhancement appears to occur in the C–N bond scission step; see ref 14a,b and the following: Satterfield, C. N.; Modell, M.; Wilkins, J. A. *Ind. Eng. Chem. Process Des. Dev.* **1980**, *19*, 154.

(16) Cordone, R.; Taube, H. *J. Am. Chem. Soc.* **1987**, *109*, 8101.

(17) Scheme I is not intended to rule out alternative mechanisms for hydride attack and ring opening.